Cell Reports
Physical Science

CellPress
OPEN ACCESS

Report

Post-positioned gas spring enables ultra-high output power of hybrid thermoacoustic electric generators

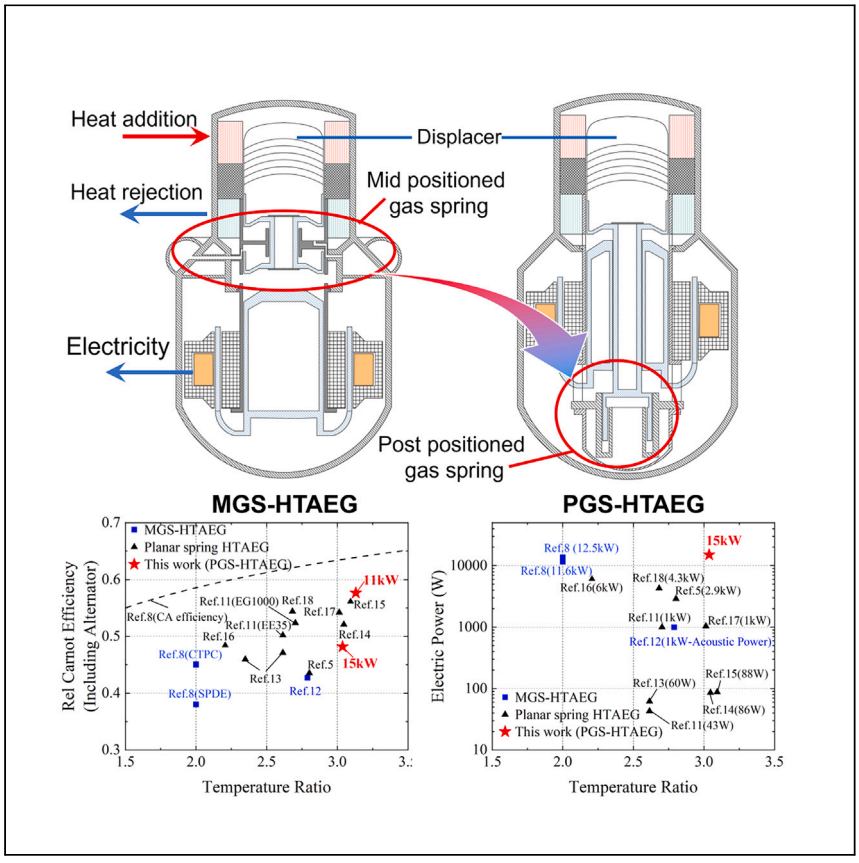

Chen et al. propose using a post-positioned gas spring to resonate the displacer in high-capacity hybrid thermoacoustic electric generators. Experiments showcase that such a configuration could achieve ultra-high output power and excellent efficiency, demonstrating that this design has significant advantages and enormous potential for application.

Yuanhang Chen, Guoyao Yu, Yanyan Chen, Shunmin Zhu, Jing Luo, Yanlei Sun, Ercang Luo

gyyu@mail.ipc.ac.cn (G.Y.)
yychen@mail.ipc.ac.cn (Y.C.)
shunmin.zhu@durham.ac.uk (S.Z.)

Highlights

A hybrid thermoacoustic electric generator with a post-positioned gas spring is proposed

A prototype of the thermoacoustic electric generator is modeled, built, and tested

15.0-kW output electric power with an efficiency of 32.5% is achieved

The prototype demonstrates the highest efficiency of 39.2% with 11.1-kW output electric power

Chen et al., Cell Reports Physical Science 5, 101835
March 20, 2024
https://doi.org/10.1016/j.xcrp.2024.101835

Cell Reports
Physical Science

CellPress
OPEN ACCESS

Report

Post-positioned gas spring enables ultra-high output power of hybrid thermoacoustic electric generators

Yuanhang Chen,[1,2] Guoyao Yu,[1,3,*] Yanyan Chen,[1,*] Shunmin Zhu,[4,5,6,*] Jing Luo,[1,2] Yanlei Sun,[1] and Ercang Luo[1,2]

SUMMARY

High-capacity hybrid thermoacoustic electric generators (HTAEGs) are ideal in different small- and micro-scale energy systems, especially in space nuclear power systems. In this work, an HTAEG with a post-positioned gas spring is proposed. To demonstrate the superiority of the gas-spring-post-positioned design on high-capacity HTAEGs, an HTAEG prototype is modeled, built, and tested from the perspective of thermoacoustics accordingly. Experimental results demonstrate an output electric power of 15.0 kW. Furthermore, it could achieve the highest efficiency of 39.2% with an output electric power of 11.1 kW. Given that a 15-kW power output is an ultra-high level on a single-piston HTAEG of this type to date, and the achieved efficiency on the prototype is also encouraging, this work marks an important milestone in the development of high-capacity HTAEGs. It also demonstrates that the gas-spring-post-positioned design has significant advantages and enormous potential for application.

INTRODUCTION

The thermoacoustic electric generator (TAEG) emerges as a promising dynamic conversion technology due to its exceptional reliability, extremely long lifespan, versatility in heat source utilization, and high intrinsic efficiency.[1] These attributes render it particularly well suited for space and submarine thermoelectric applications.[2,3] Within the TAEG family, a hybrid one (traditionally called the free-piston Stirling engine,[4] currently recognized as a generalized thermoacoustic engine[5]) that incorporates a solid mass to tune the internal acoustic field transcends the conventional gas-tuning systems in the aspects of power density and thermal-to-electrical efficiency.[6]

Most recently, dramatic progress, e.g., 16-year non-stop operation and over 39% thermal-to-electrical efficiency,[7] has stoked up the enthusiasm for the hybrid thermoacoustic electric generator (HTAEG) in space application. However, the current achievements are all confined in a rather small power level (i.e., around 100 W), not sufficient to cover various application scenarios. Scaling up to tens of kilowatt power while maintaining high reliability simultaneously is formidably challenging, and so far, there is no public literature reported on it. The main obstacle is the spring force mechanism that is imperative to tune the acoustic field. For low- and medium-power HTAEGs (ranging from tens of watts to kilowatts), planar springs are commonly employed as the spring force mechanism for their excellent compactness and radial rigidity.[8] These planar springs can be positioned either at the bounce space or compression space, resulting in two distinct designs for HTAEG. Meanwhile, both designs have been extensively

[1]Key Laboratory of Cryogenic Science and Technology, Technical Institute of Physics and Chemistry, Chinese Academy of Sciences, Beijing 100190, China

[2]University of Chinese Academy Sciences, Beijing 100049, China

[3]Institute of Optical Physics and Engineering Technology, Qilu Zhongke, Jinan 251000, China

[4]Department of Engineering, Durham University, Durham DH1 3LE, UK

[5]X (formerly Twitter): @Shunmin7

[6]Lead contact

*Correspondence: gyyu@mail.ipc.ac.cn (G.Y.), yychen@mail.ipc.ac.cn (Y.C.), shunmin.zhu@durham.ac.uk (S.Z.)

https://doi.org/10.1016/j.xcrp.2024.101835

Please cite this article in press as: Chen et al., Post-positioned gas spring enables ultra-high output power of hybrid thermoacoustic electric generators, Cell Reports Physical Science (2024), https://doi.org/10.1016/j.xcrp.2024.101835

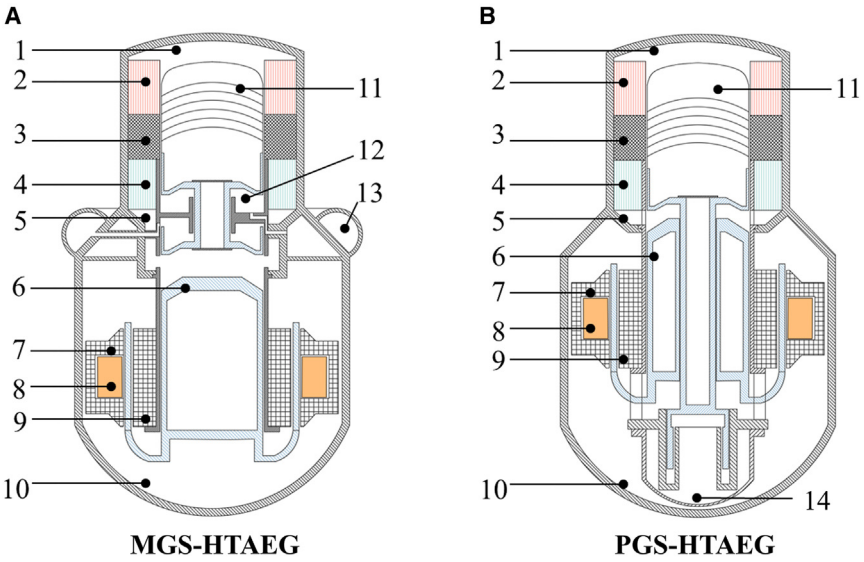

Figure 1. The schematics of hybrid thermoacoustic electric generators

(A) MGS-HTAEG: (1) expansion space (ES), (2) HHX, (3) regenerator (REG), (4) AHX, (5) compression space (CS), (6) power piston (PIS), (7) outer stator, (8) coil, (9) inner stator, (10) bounce space (BS), (11) displacer (DIS), (12) hot-end gas spring space, and (13) ambient-end gas spring space.

(B) PGS-HTAEG: (14) post-positioned gas spring space (GSS).

utilized in numerous HTAEG prototypes, with their reliability well demonstrated through ground tests.[7]

Given the escalating power demands across various sectors, especially in space nuclear power generation applications, it's imperative to develop high-capacity HTAEGs that can manage tens to hundreds of kilowatts.[9] As these HTAEGs' power capacity rises, the displacer's size and mass inevitably increase, demanding a corresponding boost in the displacer spring's stiffness to sustain its reciprocating motion. Due to the limited stiffness, conventional planar springs fall short of high-power HTAEG applications, leading to the exploration of gas springs as a promising alternative. Unlike planar springs, gas springs offer markedly higher stiffness levels, albeit with associated losses proportional to this stiffness. Importantly, this shift also mitigates certain failure modes such as mechanical spring fractures and issues like friction debris leading to regenerator blockages or piston malfunctions. Mechanical Technology Incorporated (MTI) implemented a design where the HTAEG incorporates a gas spring located at the compression space (referred to as mid-positioned gas spring HTAEG, i.e., MGS-HTAEG; see Figure 1A). Subsequently, two high-power prototypes were successfully manufactured within the NASA-funded Space Power (SP)-100 program by MTI: namely, the space power demonstrator engine (SPDE) and the component test power convertor (CTPC). The former achieved an electric power output of 17 kW and a thermal-to-electrical efficiency of 15.4% (at heating/cooling temperatures of 630 K/315 K), while the latter attained a power output of 12.5 kW and a thermal-to-electrical efficiency of 22% (at 1,050 K/525 K).[8]

Although promising results have been achieved on both SPDE and CTPC, achieving high specific power and high thermal-to-electrical efficiency simultaneously in this configuration is challenging.[10] It is important to note that the placement of the displacer gas spring within the compression space unavoidably results in an increase in dead volume, piston area, and overall engine size, hindering the conversion efficiency and

specific power.[10] Any effort to reduce the dead volume of the compression space complicates flow ducts and necessitates additional seals between different spaces, consequently leading to increased flow friction loss and a significant decline in system efficiency. To address this dilemma, a potential solution is to deploy the displacer gas spring in the bounce space instead of the compression space. This design significantly simplifies the structural complexity of the compression space, resulting in reduced flow friction loss and improved system efficiency. However, limited efforts have been made thus far to experimentally verify the feasibility of this design. To bridge this gap and demonstrate the advantages of an enhanced HTAEG with a post-positioned gas spring (post-positioned gas spring HTAEG, PGS-HTAEG), this study models, constructs, and tests a prototype incorporating this design.

RESULTS AND DISCUSSION

System configuration and numerical study

Figure 1 presents the schematics of an MGS-HTAEG and a PGS-HTAEG. The PGS-HTAEG is primarily a helium-filled pressure vessel that houses a hybrid thermoacoustic engine (HTAE) and a linear alternator (LA). The HTAE comprises an ambient heat exchanger (AHX), a regenerator, a hot heat exchanger (HHX), and a displacer. Meanwhile, the LA consists of an electromagnetic conversion circuit consisting of outer and inner stators, moving magnets, and coils, along with a power piston supported by gas bearings. Within the HTAEG, a combination of the AHX, the regenerator, and the HHX constitutes its thermoacoustic core, designed to transform external thermal energy into acoustic energy. By heating the HHX while rejecting heat from the AHX, helium within the regenerator undergoes oscillatory flow due to the thermoacoustic effect. Consequently, thermal energy is converted into acoustic energy. The displacer plays a pivotal role in modulating the acoustic field and facilitating the transfer of acoustic power. When the acoustic pressure fluctuation generated by the thermoacoustic core pushes the power piston to move reciprocating in the cylinder, the moving magnets mounted on the power piston move in a stationary coil accordingly, and the acoustic power is converted to electric power through electromagnetic induction.

A numerical model for the PGS-HTAEG was developed using the commercially available software SAGE (Note S1 and Figure S1), incorporating thermoacoustic functions and post-processing techniques. Through meticulous optimization, the dimensions of the main components were acquired and are presented in Table 1. During simulations, the PGS-HTAEG was evaluated under specific operating conditions, including a heating temperature of 550°C, a cooling temperature of 20°C, a mean pressure of 7.3 MPa, and a power piston stroke of 14.4 mm. The designed PGS-HTAEG demonstrates the ability to generate 15.3 kW of electric power while consuming 38.3 kW of input heating power, resulting in an efficiency of 39.5%.

Figure 2A shows a comparison of the available energy losses (AE losses) occurring in the core components of a PGS-HTAEG and an MGS-HTAEG. Numerical analysis further demonstrates that the PGS-HTAEG, featuring its intractable gas spring, achieves a remarkable thermal-to-electrical efficiency enhancement of 10.6% in comparison to an MGS-HTAEG. In the MGS-HTAEG, the stiffness of the gas spring is equivalent to that of the PGS-HTAEG's post-positioned gas spring but includes additional seal structures. Analyzing Figure 2A reveals that the friction losses in the gas spring space of the MGS-HTAEG are significantly higher than those in the PGS-HTAEG. This discrepancy arises because the mid-positioned spring is confined within limited space, resulting in a more complex seal and flow path compared with the post-positioned gas spring.

Table 1. Dimensions of the main component

Component	Specification	Value
ES	volume (L)	0.57
HHX	heat exchanger type	rectangular fin
	axial length (mm)	77
	fin number	650
REG	regenerator type	random fiber
	axial length (mm)	60
	equivalent diameter (mm)	202
	porosity	90%
AHX	heat exchanger type	shell and tube
	axial length (mm)	70
	number of tubes	990
	diameter, facing the expansion space (mm)	150
DIS	rod diameter (mm)	52
	moving mass (kg)	3.25
	gas spring piston diameter (mm)	90
GSS	volume (L)	1.25
CS	volume (L)	0.55
PIS	equivalent diameter (mm)	140.7
	moving mass (kg)	12.65
LA	transduction coefficient (N/A)	260
	magnetic spring stiffness (kN/m)	300
	winding resistance (Ω)	0.54
BS	volume (L)	19.43

Furthermore, the AE losses that occur in the AHX, regenerator, and displacer of the PGS-HTAEG are also lower than those in the MGS-HTAEG. The reduction in available energy losses within both the AHX and regenerator of the PGS-HTAEG can be attributed to the decrease in available energy loss (AEQw as symbolized in Figure 2A) within these components. This reduction is mainly due to the lower dead volume of the compression space in the PGS-HTAEG compared with the MGS-HTAEG. Moreover, the decreased amplitude of the displacer in the PGS-HTAEG leads to a lower AEdamp in the displacer compared to the MGS-HTAEG.

To gain a comprehensive understanding of the energy conversion and transfer processes within the PGS-HTAEG, Figure 2B illustrates the power flow distribution. It's clear that the acoustic power from the compression space is amplified in the regenerator and then transfers to the expansion space, where the acoustic power drives the back-and-forth motion of the displacer, while simultaneously transferring the acoustic power to the compression space and bounce space. The acoustic power transferred to the compression space is divided into two distinct parts. Firstly, a portion of the acoustic power (15.4 kW) drives the power piston in a reciprocating motion, subsequently converting it into electrical power through the LA. Secondly, another portion of the acoustic power (19.3 kW) flows into the AHX, where it perpetuates the cycle. A notable characteristic of the PGS-HTAEG is the alteration of the acoustic field in the bounce space, as depicted in Figure 3. In this configuration, a substantial amount of acoustic power (1.3kW, accounting for 7.8% of the total output of acoustic power) is transported from the expansion space to the bounce space by the displacer. This transferred acoustic power then acts upon the power piston, ultimately being converted into electric power. This insight into the power flow dynamics underscores the unique energy conversion mechanisms in the PGS-HTAEG, illustrating its potential for enhanced performance compared to traditional HTAEG designs.

Please cite this article in press as: Chen et al., Post-positioned gas spring enables ultra-high output power of hybrid thermoacoustic electric generators, Cell Reports Physical Science (2024), https://doi.org/10.1016/j.xcrp.2024.101835

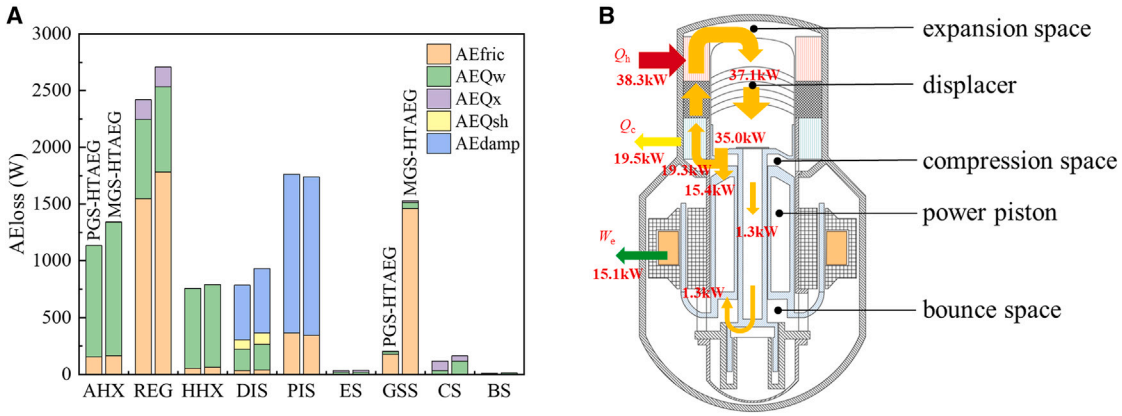

Figure 2. Available energy losses distribution and energy flow in the PGS-HTAEG

(A) Comparison of available energy losses (AE losses) that occur in the core components of the PGS-HTAEG and MGS-HTAEG.

(B) The energy flow in the PGS-HTAEG.

Experimental performance evaluation

Following the completion of the thermodynamic and dynamic design, a prototype of PGS-HTAEG was developed. Figure 3A shows the schematic diagram of the test system, while Figure 3B displays a photograph of the actual prototype. The test system comprises the generator prototype, along with a heating sub-system, a cooling sub-system, a load sub-system, and a measurement sub-system. In experiments, electrical heaters were employed to supply heating power to the HTAE. Cooling water from an industrial water chiller was used to cool the AHX with the cooling water volume flow rate and outlet water temperature adjusted to maintain the AHX wall temperature. Temperature measurements were carried out using K-type thermocouple-thermometers (with an accuracy of 1°C) for the HHX wall temperatures. Inlet and outlet water temperatures at the AHX were measured using two PT-100 platinum resistance thermometers (with an accuracy of 0.15°C + 0.002|t|°C, t is the test value). To assess the performance of the LA, the output voltage and current were measured using a differential voltage probe (Pintech, model N1070APro, with an accuracy of 0.5%) and a current probe (Pintech, model PT710-A, with an accuracy of 4%), respectively. The input heating power of the HTAE was calculated based on the measured voltage and current (both with an accuracy of 0.5%) of the heating sub-system. In addition, the strokes of the power piston and the displacer were measured using two linear variable differential transformers (LVDTs) from Shenzhen Soway (model SDVG36-40C, with a full scale [FS] of 40 mm and an accuracy of 1% FS).

In the experiments, helium was utilized as the working gas in the HTAEG, with a charge pressure of 6.4 MPa. Throughout the experiments, the outlet water temperature of the industrial water chiller was maintained at 20°C with a fluctuation range of 5°C. Additionally, the stroke of the power piston and the wall temperature of the HHX (heating temperature) were adjusted by controlling the rheostat value and input heating power. It is worth noting that, for safety reasons, the heating temperature was kept below 650°C.

Figure 4A gives the output electric power and thermal-to-electrical efficiency ($\eta_l = W_e/Q_h$, where W_e represents the electric power output of the LA, and Q_h corresponds to the input heating power of the HTAE) as a function of the input heating power for different rheostat values. It is observed that reducing the rheostat value leads to both higher output electric power and efficiency at a constant input heating power. Specifically, by decreasing the rheostat value to 42 Ω with an input heating power of 28.3 kW, the prototype achieved

Please cite this article in press as: Chen et al., Post-positioned gas spring enables ultra-high output power of hybrid thermoacoustic electric generators, Cell Reports Physical Science (2024), https://doi.org/10.1016/j.xcrp.2024.101835

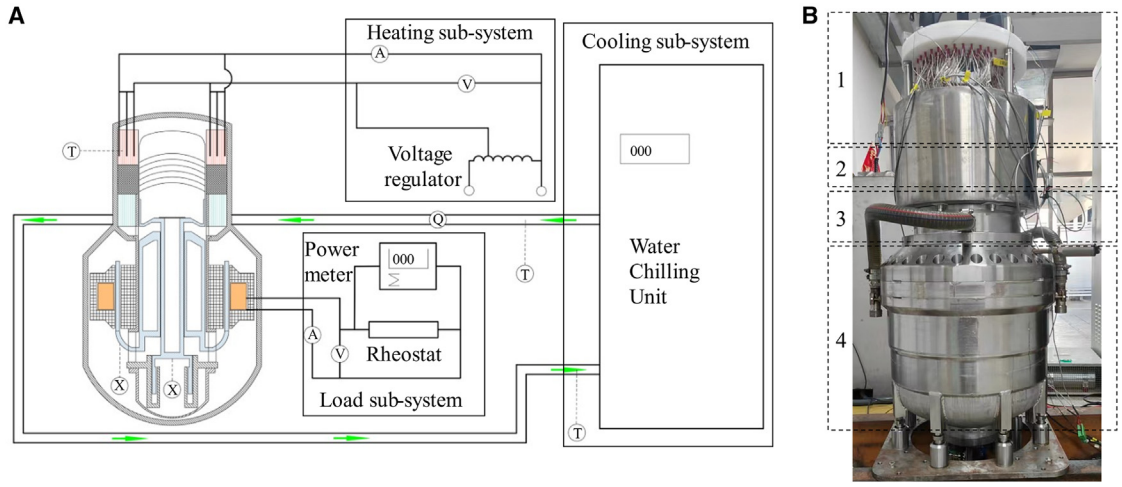

Figure 3. Configuration and photograph of the experimental system

(A) Schematic diagram of the test system for the PGS-HTAEG prototype ("T" represents temperature measurement, "X" represents LVDT, "A" stands for current probe, "V" stands for voltage probe, and "Q" stands for flowmeter).

(B) Photograph of the PGS-HTAEG prototype: (1) HHX with electric heaters, (2) regenerator, (3) HX, and (4) LA.

a maximum efficiency of 39.2% and an output electric power of 11.1 kW. Most importantly, with a rheostat value of 45 Ω and an input heating power of 46.4 kW, a maximum output electric power of 15.0 kW was obtained with an associated efficiency of 32.5%. Regarding each fixed rheostat value (50 Ω and 80 Ω), there is a slight increase in efficiency as the input heating power rises.

The experimental results, as depicted in Figure 4A, exhibit a good agreement with the simulation results, and the deviations remain within a range of 10%. Nevertheless, as the rheostat value decreases, there is a slight augmentation in the discrepancy, which can be attributed to an increased equivalent mechanical resistance inflicted by intensified pressure fluctuation and gas temperature.

Figure 4B presents a comparison of the relative Carnot efficiency ($\eta_{II} = \eta_I/(1\text{-}T_0/T_h)$, where T_0 represents the ambient-end temperature and T_h is the heating temperature) of the HTAEG prototype with other prototypes reported in published papers.[5,8,11–18] The PGS-HTAEG prototype developed in this study demonstrates an exceptional relative Carnot efficiency of 57.7%, surpassing all previously reported HTAEG prototypes documented in the literature. Furthermore, Figure 4C illustrates that the electric power output of 15.0 kW attained on a single-piston HTAEG is unparalleled within published papers.

In conclusion, this study has developed an improved design for high-capacity HTAEGs by incorporating a post-positioned gas spring to meet the requirement of high specific power and high efficiency. Compared to an HTAEG with a gas spring located in the compression space, the improved HTAEG demonstrates a 10.6% increase in efficiency. To validate the superiority of this unique design, a prototype is modeled, constructed, and tested.

The experimental results demonstrate significant achievements. At a heating temperature of 604.3°C, the prototype achieves a maximum output electric power of 15.0 kW with an efficiency of 32.5%. Moreover, at a heating temperature of 635.0°C, the prototype attains a maximum efficiency of 39.2% and an output electric power of 11.1 kW. The achieved power level of 15 kW by a single-piston HTAEG stands as the highest reported

Please cite this article in press as: Chen et al., Post-positioned gas spring enables ultra-high output power of hybrid thermoacoustic electric generators, Cell Reports Physical Science (2024), https://doi.org/10.1016/j.xcrp.2024.101835

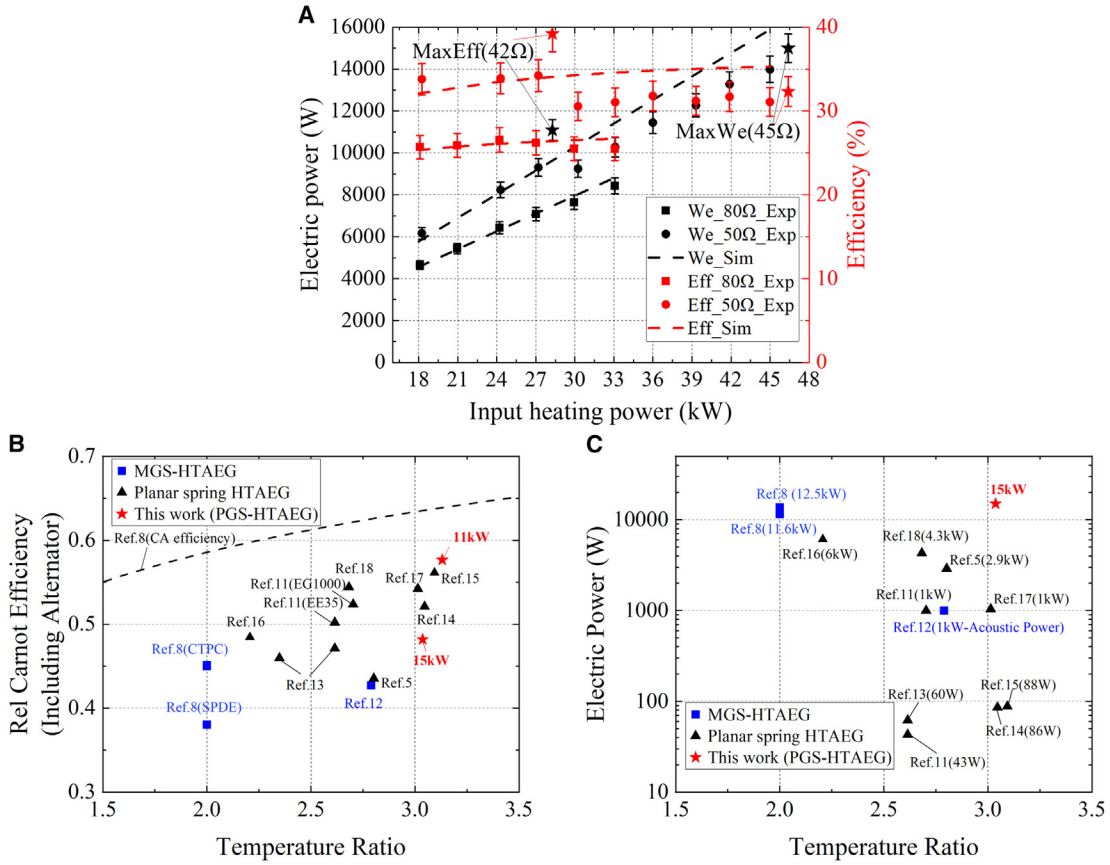

Figure 4. Experiment results of the prototype

(A) The electric power and efficiency versus input heating power under various electric resistances (the error bars mean the measuring accuracy).

(B and C) Comparison of the relative Carnot efficiency (B) and the electric power output (C) of the HTAEG prototype with other prototypes presented in published papers.

in published literature, while its efficiency culminates in developed HTAEG prototypes. These results indicate a promising application potential for the HTAEG with a post-positioned gas spring, particularly in space nuclear power systems.

Moving forward, our future research will delve deeper into the operational characteristics of the HTAEG with a post-positioned gas spring. We aim to develop an opposing system with two such HTAEGs, if feasible, to mitigate system vibrations.

EXPERIMENTAL PROCEDURES

Resource availability

Lead contact

Further information and requests should be directed to the lead contact, Shunmin Zhu (shunmin.zhu@durham.ac.uk).

Materials availability

This study did not generate new unique materials.

Data and code availability

The data that support the findings of this study are available from the corresponding author upon reasonable request.

CellPress OPEN ACCESS

Cell Reports Physical Science Report

SUPPLEMENTAL INFORMATION

Supplemental information can be found online at https://doi.org/10.1016/j.xcrp.2024.101835.

ACKNOWLEDGMENTS

This research was financially supported by the National Key Research and Development Program of China (no. 2021YFC28026003) and National Natural Science Foundation of China (no. 51876214 and no. 52306031). This work was also supported by the European Union's Marie Skłodowska-Curie Actions Individual Fellowship (no. MSCA-IF-101026323). The authors greatly thank Mr. Ruifeng An, Mr. Ying Ma, Mr. Bin Liu, Mr. Jianmin Fang, Mr. Yangbin Cheng, et al. for their invaluable engineering support in prototype manufacturing and experiments.

AUTHOR CONTRIBUTIONS

Conceptualization, G.Y.Y., Y.Y.C., and S.M.Z.; methodology, G.Y.Y. and Y.Y.C.; investigation, Y.H.C., J.L., and Y.L.S.; writing – original draft, Y.H.C.; writing – review & editing, S.M.Z. and G.Y.Y.; funding acquisition, G.Y.Y., Y.Y.C., and S.M.Z.; supervision, G.Y.Y., Y.Y.C., and E.C.L.

DECLARATION OF INTERESTS

The authors declare no competing interests.

Received: November 27, 2023
Revised: January 10, 2024
Accepted: January 25, 2024
Published: February 21, 2024

REFERENCES

1. Zhu, S., Yu, G., Liang, K., Dai, W., and Luo, E. (2021). A review of Stirling-engine-based combined heat and power technology. Appl. Energy *294*, 116965. https://doi.org/10.1016/j.apenergy.2021.116965.

2. Schriener, T.M., and El-Genk, M.S. (2021). Thermal analyses of high-power advanced thermoacoustic radioisotope power system for future space exploration missions. Nucl. Eng. Des. *385*, 111504. https://doi.org/10.1016/j.nucengdes.2021.111504.

3. Tward, E. (2003). Thermoacoustic Space Power Converter (AIP Conference Proceedings (AIP)), pp. 656–661. https://doi.org/10.1063/1.1541352.

4. Beale, W.T. (1969). Free Piston Stirling Engines - Some Model Tests and Simulations, p. 690230. https://doi.org/10.4271/690230.

5. Zhu, S., Yu, G., O, J., Xu, T., Wu, Z., Dai, W., and Luo, E. (2018). Modeling and experimental investigation of a free-piston Stirling engine-based micro-combined heat and power system. Appl. Energy *226*, 522–533. https://doi.org/10.1016/j.apenergy.2018.05.122.

6. Bi, T., Wu, Z., Zhang, L., Yu, G., Luo, E., and Dai, W. (2017). Development of a 5 kW traveling-wave thermoacoustic electric generator. Appl. Energy *185*, 1355–1361. https://doi.org/10.1016/j.apenergy.2015.12.034.

7. Wilson, S. (2023). Development of Stirling Convertors for Radioisotope and Fission Power Systems. In Nuclear and Emerging Technologies for Space (NETS).

8. Mason, L.S., and Schreiber, J.G. (2007). A Historical Review of Brayton and Stirling Power Conversion Technologies for Space Applications. Space Nuclear Conference.

9. Mason, L.S. (2006). A Comparison of Fission Power System Options for Lunar and Mars Surface Applications. AIP Conf. Proc. *813*, 270–280. https://doi.org/10.1063/1.2169203.

10. Luo, J., Zhang, L., Chen, Y., Sun, Y., Yu, G., Hu, J., and Luo, E. (2023). Numerical study on a free-piston Stirling electric generator with a gas-spring-postpositioned displacer for high-power applications. Energy *271*, 127023. https://doi.org/10.1016/j.energy.2023.127023.

11. Kim, S., Huth, J., and Wood, J. (2005). Performance Characterization of Sunpower Free-Piston Stirling Engines. In 3rd International Energy Conversion Engineering Conference (American Institute of Aeronautics and Astronautics). https://doi.org/10.2514/6.2005-5540.

12. Schreiber, J. (1983). Testing and performance characteristics of a 1-kW free piston Stirling engine. NASA STI/Recon Technical Report N *83*, 25036.

13. Furlong, R., and Shaltens, R. (2000). Technology assessment of DoE's 55-We Stirling technology demonstrator convertor (TDC). In 35th Intersociety Energy Conversion Engineering Conference and Exhibit (American Institute of Aeronautics and Astronautics). https://doi.org/10.2514/6.2000-3018.

14. Wood, J.G. (2005). Advanced 80 We Stirling Convertor Development Progress (AIP Conference Proceedings (AIP)), pp. 688–698. https://doi.org/10.1063/1.1867188.

15. Wilson, S.D., and Poriti, S. (2010). Advanced Stirling Convertor Testing at NASA Glenn Research Center. In 8th International Energy Conversion Engineering Conference. IECEC 2010).

16. Wood, J.G., and Stanley, J. (2016). Free-Piston Stirling Power Conversion Unit for Fission Power System, Phase II Final Report.

17. Jia, Z., Wang, R., Hu, J., Zhang, L., Wu, Z., Chen, Y., and Luo, E. (2022). Study on the coupling between engine and alternator in a free-piston Stirling generator. Appl. Therm. Eng. *217*, 119222. https://doi.org/10.1016/j.applthermaleng.2022.119222.

18. Jiang, Z., Yu, G., Zhu, S., Dai, W., and Luo, E. (2022). Advances on a free-piston Stirling engine-based micro-combined heat and power system. Appl. Therm. Eng. *217*, 119187. https://doi.org/10.1016/j.applthermaleng.2022.119187.